Neural Network Based Saturation Model for Round Rotor Synchronous Generator

S. Pillutla, Student Member, IEEE A. Keyhani, Fellow, IEEE
Department of Electrical Engineering,
The Ohio State University
Columbus, OH 43210 USA

Abstract: This paper presents an artificial neural network (ANN) based technique to model saturation for a round rotor synchronous generator. The effects of excitation level, rotor angle, and real power generation on generator saturation are included in the modeling process. To illustrate the technique, small excitation disturbance tests are conducted on a 7.5 kVA, 240V, 60 Hz. round rotor synchronous generator at various levels of excitation and loading. The small excitation disturbance responses are processed by a recursive maximum likelihood algorithm to yield estimates of mutual inductances L_{ad} and L_{aq} at each operating condition. By developing a suitable training pattern, variables representative of generator operating condition are mapped to mutual inductances L_{ad} and L_{aq}. The developed models are validated with measurements not used in the training process and with large disturbance responses.

Keywords: Synchronous generators, modeling, parameter estimation, neural networks.

I. INTRODUCTION

Accurate stability analysis requires the precise modeling of generator saturation – a complex phenomenon involving loading conditions, excitation levels, and the relative position of the rotor with respect to the magnetic axis of the stator winding. This is especially true in the case of round-rotor synchronous generators where saturation can be significant both in the direct and quadrature axis [1].

In recent years, saturation factor methods have been introduced to accurately model machine saturation [2-10,15]. These methods involve suitably modifying the d- and q-axis mutual inductances, which are essentially functions of magnetizing currents in the core, air-gap mmf, or the air-gap voltage (flux). As pointed out by Dandeno, El-Serafi, Shackshaft and other researchers, the extent of saturation in the d- and q-axis is not identical; saturation in the q-axis is much greater than that in the d-axis due to the presence of rotor teeth along the magnetic path in the q-axis [3,4]. In reference [6], de-Mello and Hannett proposed a saturation model based on the air-gap voltage.

PE-161-EC-0-08-1998 A paper recommended and approved by the IEEE Electric Machinery Committee of the IEEE Power Engineering Society for publication in the IEEE Transactions on Energy Conversion. Manuscript submitted December 1, 1997; made available for printing August 14, 1998.

In order to take into account that saturation changes with different rotor positions along the air-gap, El-Serafi [7] introduced saturation factors which are varied according to the resultant mmf in the d- and q-axis. The effects of loading on the saturation trajectory were studied by Shackshaft [3] who proposed a model in which the conventional air-gap voltage magnitude dependent saturation functions are modified according to the air-gap voltage angle as well. In reference [8], Minnich *et al* proposed a finite-element-method (FEM) to model machine saturation. In most of the current literature on machine saturation modeling, the independent variables used in representing the non-linear variations of the saturation factors are either the terminal voltage, current, or a combination of these quantities including the phase angle. In addition, the leakage reactances, sub-transient reactances, and Potier reactances are often incorporated into these independent variables in order to reflect the dependency of saturation factors on the machine power angles under loaded conditions. Due to the high dimensionality of variables, only some but not all of the physical factors that are known to influence saturation are considered.

Several authors have recently investigated the use of generator on-line operating data for identifying machine model parameters [15-19]. These techniques employ advanced system identification algorithms for parameter estimation purposes. From a viewpoint of accurate parameter estimation, on-line techniques are considered realistic because the operating data used in the estimation procedure contains embedded information representative of the effects of machine operating condition, including saturation, thermal, and rotational effects.

In this study, an artificial neural network is used to represent saturated mutual inductances as a multi-dimensional non-linear function of operating condition dependent machine variables. This scheme can estimate the non-linear functional relationship between machine variables and saturated mutual inductances by learning from user-provided experimental data. It is not necessary to determine the shape of the mapping beforehand. Instead, the ANN extracts the shape of the non-linear function from training data. In reference [14], saturation models for a salient pole synchronous generator were developed. In this paper, a similar methodology is applied to establish ANN saturation models for a round-rotor synchronous generator.

II. MACHINE MODEL DESCRIPTION AND PROBLEM FORMULATION

The structure of the synchronous machine model used in this study (Model 3'.3) is shown in reference [20] and is based on the reciprocal per-unit system. For discrete-time systems, the coupled state-space representation of this model can be written as:

$$X(k+1) = A(\theta)\cdot X(k) + B(\theta)\cdot U(k) + w(k)$$
$$Y(k+1) = C\cdot X(k+1) + v(k+1) \quad (1)$$

$w(k)$ and $v(k)$ denote the process and measurement noise, respectively. In addition,

$$X = [i_q \;\; i_d \;\; i_{1q} \;\; i_{2q} \; i_{3q} \;\; i_{1d} \;\; i_{fe1d} \;\; i_{fd}^*]^T;$$
$$U = [v_q \; v_d \;\; v_{fd}^*]^T;$$
$$Y = [i_q \;\; i_d \;\; i_{fd}^*]^T;$$

$$\theta = [R_a \;\; R_{fd}^* \;\; R_{1d} \;\; R_{fe1d} \;\; L_l \;\; L_{ad} \;\; L_{fd} \;\; L_{1d} \;\; L_{fe1d} \;\; a$$
$$R_{1q} \;\; R_{2q} \;\; R_{3q} \;\; L_{aq} \;\; L_{1q} \;\; L_{2q} \;\; L_{3q}]^T;$$

The A and B matrices and the parameter vector θ are given in reference [20]. In the above formulation, all parameters are in actual units. Also, it is assumed that the machine power angle, δ, is available for measurement. Variables v_d, v_q, i_d, i_q represent generator d- and q-axis terminal voltages and terminal currents respectively. Also, i_{fd}^* is the field winding current in ampere, v_{fd}^* is the field voltage in volts, both quantities measured on the field side of the generator. R_{fd}^* is the field winding resistance in ohm as measured on the field side. i_{fd}, v_{fd}, and R_{fd} denote corresponding transformed quantities on the stator side of the generator through the field-to-stator turns ratio a. All other variables and parameters are referred to the stator and are in actual units.

The ANN based generator saturation models are established in two stages. In Stage 1, small excitation disturbance data is used to identify linear machine parameters over a wide range of operating conditions. The saturated mutual inductances L_{ads} and L_{aqs} (the subscript s is used to denote saturated values of mutual inductances L_{ad} and L_{aq} respectively) are estimated at different levels of excitation and power generation. In Stage 2, small excitation disturbance responses obtained over various operating conditions are mapped to the estimated saturated mutual inductances using a multi-layer feed-forward ANN.

In order to validate the established saturation models, simulation studies are performed and the results are compared against actual measurements under large excitation disturbances. In these studies, measured terminal-voltages and field voltage are used to excite the machine model to obtain terminal-currents and field current. The simulated currents are compared against corresponding experimental currents.

III. ESTIMATION OF SATURATED MUTUAL INDUCTANCES

The first stage of the estimation process involves the estimation of saturated mutual inductances, L_{ads} and L_{aqs} from small excitation disturbance responses. Also estimated are the armature resistance R_a, field-to-stator turns ratio a, and the field resistance R_{fd}^*.

Note that since the disturbance is small, the rotor speed, ω_r is assumed to be essentially constant at synchronous speed. Furthermore, since the machine is connected to a transformer through the power system, the rate of change of flux linkages can be ignored under small disturbance conditions [19]. Hence, the output equations for the machine models at time instant k are written as:

$$\begin{cases} v_d(k) = -R_a i_d(k) - \omega_r(k)\Phi_q(k) \\ v_q(k) = -R_a i_q(k) + \omega_r(k)\Phi_d(k) \end{cases} \quad (2)$$

where Φ_d and Φ_q represent the stator d- and q-axis flux linkages. At steady state and small excitation disturbance conditions, rotor body currents are practically negligible. Thus, equation (2) can be represented by a linear model as:

$$Y(k) = H(k)\,\Theta(k) + v(k) \quad (3)$$

In equation (3), $Y=[v_d \;\; v_q]^T$; $\Theta = [R_a \;\; a\,L_{ads} \;\; L_{qs} \;\; L_{ds}]^T$ and v represents the measurement noise. Without rotor body dynamics under steady state conditions, the matrix H is a function of two-axis terminal currents and field current given by

$$H = \begin{bmatrix} -i_d & 0 & \omega_r i_q & 0 \\ -i_q & \frac{2}{3} i_{fd}^* & 0 & -\omega_r i_d \end{bmatrix} \quad (4)$$

Using a record of input-output observations Y and H, a recursive estimation procedure [19] is used to estimate the parameter vector Θ. The field resistance R_{fd}^* can be computed using the measured v_{fd}^* and i_{fd}^* at the steady-state condition. The saturated mutual inductances L_{ads}, L_{aqs} are estimated from L_{ds}, L_{qs} by assuming the stator leakage inductance L_l as equal to 0.0011H. This value of L_l is obtained from standstill time-domain response testing of the test generator as explained in reference [20]. An elaborate discussion of the estimation process from on-line test data is provided in references [14, 19]. Table 1 lists the linear model parameters of the synchronous generator estimated by conducting small excitation disturbance tests with the machine operating at light load and under-excited conditions.

Table 1: Linear Model Parameters

Parameter	Estimate
R_a	0.4205
L_l	0.0011
L_d	0.0559
L_q	0.0464
R_{fd}	0.5589
a	1.1971

Resistance (Ω), Inductance (H).

Next, small excitation disturbance tests are conducted over a wide range of operating conditions to estimate the saturated mutual inductances L_{ads} and L_{aqs} at various levels of excitation and power generation.

It is desirable to graphically visualize the variation of L_{ads} and L_{aqs} as a function of all the machine variables (v_d, v_q, i_d, i_q, v_{fd}^*, and i_{fd}^*) representative of machine operating condition. However, such a visualization is not possible because we can at most represent this variation in three-dimensions. But if we consider some of the machine variables to be constant, the variation of L_{ads} and L_{aqs} can be portrayed in terms of the remaining variables. For instance, Fig. 1 depicts the variation of L_{ads} and L_{aqs} as a function of generator rotor-angle and average field-current at the machine's rated terminal voltage. It must be understood that at rated terminal voltage, the field-current and the power angle are representative of the operating condition of the generator. At under-excited conditions, when the generator is delivering small amounts of real power, machine saturation is small. However, at large values of field current and rotor angle when the machine is delivering a substantial amount of real power, the extent of saturation is quite considerable.

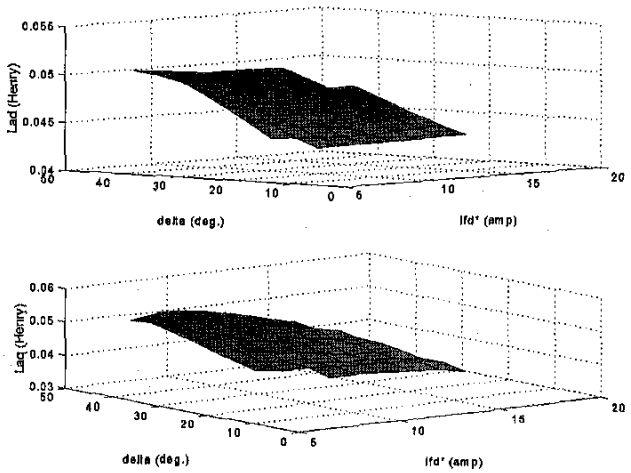

Fig. 1: Variation of saturated mutual inductances as a function of rotor angle, δ, and field current, I_{fd}^*

IV. NEURAL NETWORK SATURATION MODEL

The multi-layer feedforward perceptron has often been used in system identification studies. This network, in general, consists of a number of basic computational units called processing elements connected together to form multiple layers. Fig. 2 shows the schematic of a typical processing element which forms a weighted sum of its inputs and passes the result through a non-linear transformation (also called transfer function) to the output. The transfer function may also be linear in which case the weighted sum is propagated directly to the output path. The multi-layer perceptron used in this paper consists of processing elements arranged in three distinct layers. Data presented at the network's input layer, is processed and propagated through a hidden layer, to the output layer. Training a network is the process of iteratively modifying the strengths (weights) of the connecting links between processing elements as patterns of inputs and corresponding desired outputs are presented to the network.

In this work, the mathematical relationship between the input and output patterns can be described as:

$$\begin{cases} L_{ads} = N_d(v_d \quad v_q \quad i_d \quad i_q \quad i_{fd}^*) \\ L_{aqs} = N_q(v_d \quad v_q \quad i_d \quad i_q \quad i_{fd}^*) \end{cases} \tag{5}$$

where N_d and N_q are non-linear neural network mappings to be established. The field voltage v_{fd}^* is not included as part of the mapping because it is simply a scaled version of the field current i_{fd}^* obtained during small excitation disturbance testing.

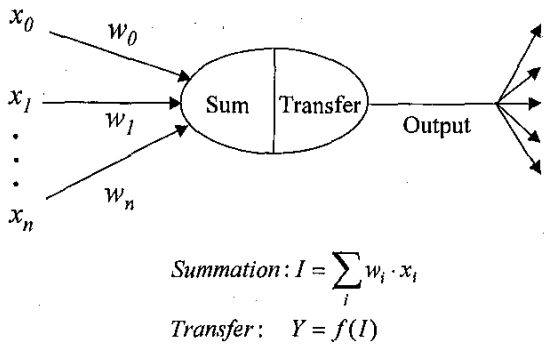

Fig. 2: Schematic diagram of basic processing element.

The multi-layer feed-forward perceptron used in this study is shown in Fig. 3 and consists of 5 processing elements in the input layer, corresponding to each generator variable given in equation (5). A single processing element in the output layer corresponds to the mutual inductance (L_{ads} or L_{aqs}) being modeled. The number of elements in the hidden layer is arbitrarily chosen depending on the complexity of the mapping to be learnt. A hyperbolic tangent (tanh) transfer function is used in all hidden layer elements, while all elements in the input layer and output layer have linear (1:1) transformations. The back-propagation algorithm [26,27] is used to train the neural network such that the sum squared error, E, between actual network outputs, O, and corresponding desired outputs, ζ, is minimized over all training patterns μ.

$$E = \sum_{\mu} [\zeta_\mu - O_\mu]^2 \tag{6}$$

After estimating the non-linear mapping N_d (or N_q) of equation (5) in terms of the neural network, the network output $L_{ads,est}$ (or $L_{aqs,est}$) is computed from the 5x1 input vector P according to the following equation:

$$L_{ais,est} = W_2 \cdot \tanh(W_1 \cdot P + B_1) + B_2 \tag{7}$$

where the term $L_{ais,est}$ denotes the estimated saturated mutual inductance (i = d- or q-axis). W_2 denotes the matrix of connecting weights from the hidden layer to the output layer. W_1 is the weight matrix from the input-layer to the hidden-layer. If

there are m processing elements in the hidden layer, W_2 is of size $1xm$, and W_1 is of size $mx5$. Bias terms B_2 and B_1 are used as connection weights from an input with a constant value of one. B_2 and B_1 denote the $1x1$ and $mx1$ bias vectors from the bias to the output-layer, and from the bias to the hidden-layer respectively. The task of training is to determine the matrices W_1, W_2, and bias vectors B_1, B_2.

The training patterns required to train the neural network models are obtained through an experimental arrangement and on-line data acquisition process described in reference [19]. Data is obtained by staging small excitation disturbance tests wherein the magnitude of the external input ΔV_{ref} is between 2% and 5% of the excitation reference voltage, V_{ref}. Such tests do not significantly affect the overall operating status of the system, and are feasible even on large utility generators.

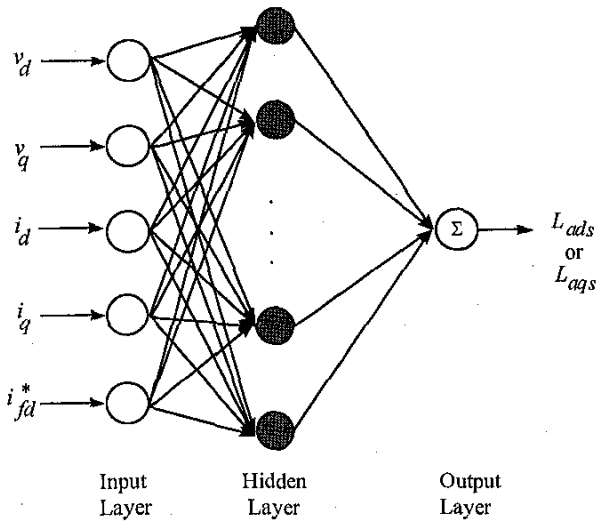

Fig. 3: Multilayer Feedforward ANN Based Generator Saturation Model

V. ANN SATURATION MODEL DEVELOPMENT

In this section, a multidimensional non-linear neural network mapping is established to map small excitation-disturbance responses to a set of experimentally obtained saturated mutual inductances. Using the identified mutual inductances obtained over various operating conditions as the output pattern, and measured machine responses as the input pattern, the machine saturation model can be established by using two multilayer feedforward ANNs (one for each orthogonal axis) trained by the back-propagation algorithm. Let the input pattern P be given by:

$$P = \left[V_d \quad V_q \quad I_d \quad I_q \quad I^*_{fd} \right]^T$$

where V_d, V_q, I_d, I_q, I_{fd}^* represent the per-unitized average values of the orthogonal axis voltages and currents. Also, let the output pattern for each mutual inductance ANN model be the per-unitized L_{ads} and L_{aqs}. It should be noted that per-unitized values are used instead of actual values to avoid plasticity problems that can occur during training. For instance, it was recognized that even with small weights in the network, the summations can be very large. The derivatives of the tanh function can be close to zero at large summation values. Since the derivative is a multiplier in the back-propagation weight update equations, learning stops for processing elements with large summation values. This phenomenon wherein the network loses its ability to react to any new data is referred to as plasticity [26].

In this study, the training set consisted of 42 five-dimensional input patterns for ANN model. The sum squared error criterion for training was set at 0.01. The number of elements in the hidden layer of the ANN models were established through a trial-and-error procedure. Initially one processing element was used in the hidden layer of each ANN. Using such a 5-1-1 structure, we attempted to train each ANN model but failed to achieve convergence. By gradually increasing the number of elements in the hidden layer, we were able to train the networks such that the sum squared error criterion is met. Convergence could be achieved by using a large number of processing elements in the hidden layer. However there is a danger of over-fitting i.e, the network memorizes the patterns used in training but cannot generalize and respond accurately to previously unseen patterns. Thus, after training, it is necessary to use an independent cross-validation data set comprising of patterns that are not part of the training set. Using a cross-validation set, it is possible to judge whether the networks are able to generalize properly. It must be remembered that the weights of the ANN models are adjusted only during training, and not during cross-validation or testing. Using the above procedure, we found the optimal number of elements in the hidden layer for the d- and q-axis saturation models to be equal to 5 and 10 respectively.

The performance of the ANN saturation models established above are compared against a cross-validation data set comprising of per-unitized average values of orthogonal axis voltages and currents obtained from small excitation disturbance testing, not previously included in the training set. 20 such patterns are presented to the trained ANN models. The values of mutual inductances estimated by the saturation models are compared with actual values obtained by using the procedure outlined in section III. As shown in Figures 4 and 5, the ANN saturation models can correctly interpolate between patterns not used in the training process.

VI. ANN SATURATION MODEL VALIDATION

In order to verify the accuracy of the ANN saturation models under large disturbance conditions, two large excitation disturbance tests were conducted. Using measured voltages v_d, v_q and v_{fd}^*, the currents i_d, i_q, and i_{fd}^* are simulated (see equation (1)) and compared against corresponding measured currents. For simulation purposes, it is necessary to consider the rate of change of stator flux linkages. Also, the rotor speed variation is included in the computation. The simulation details are presented below.

Using a record of experimentally measured input-output data (v_d, v_q, i_d, i_q, i_{fd}^*) obtained during a large disturbance transient event, the d- and q-axis stator flux-linkages are first computed.

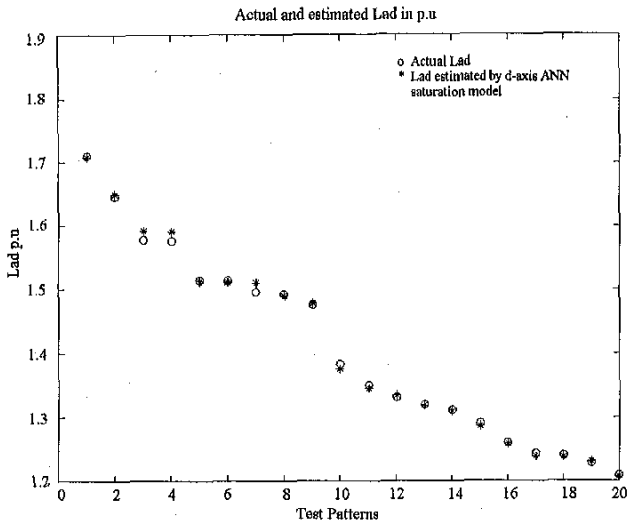

Fig. 4: Actual and ANN estimated generator mutual inductances for the L_{ads} saturation model.

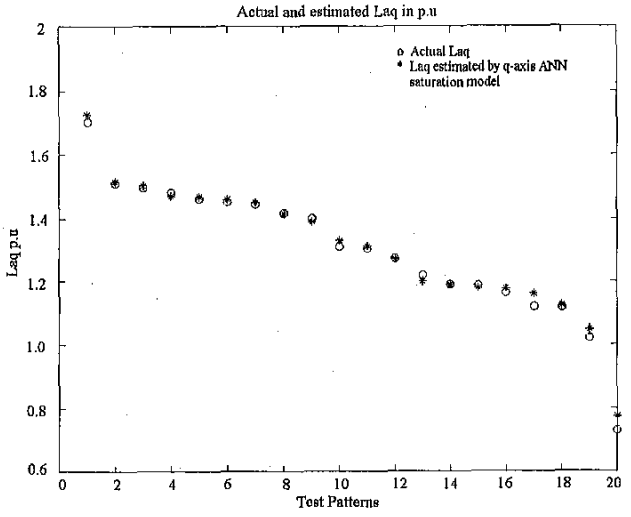

Fig. 5: Actual and ANN estimated generator mutual inductances for the L_{aqs} saturation model.

This is done by arranging the machine stator voltage equations in a state-space form to solve for the flux linkages Φ_d and Φ_q using numerical integration:

$$X(k+1) = A \cdot X(k) + B \cdot U(k) \tag{8}$$

where $X = [\Phi_d \quad \Phi_q]^T$. Matrices A, B, U are defined in Appendix A.1. If I_d, I_q, V_d, V_q correspond to the steady-state stator d- and q-axis currents and voltages respectively, the following equations may be used to compute initial flux linkages at steady state (prior to a transient disturbance):

$$\begin{cases} \Phi_d = \dfrac{R_a I_q + V_q}{\omega_r} \\ \Phi_q = -\dfrac{R_a I_d + V_d}{\omega_r} \end{cases} \tag{9}$$

In the above equation, R_a is obtained from Table 1. With estimates of stator d- and q-axis flux-linkages, the speed-voltage terms appearing in the d- and q-axis equivalent circuits viz., $\Phi_q\omega_r$ and $\Phi_d\omega_r$ are calculated (see Appendix A.1). This would facilitate in de-coupling equation (1) into two subsystems, one for each orthogonal axis:

For the d-axis model,

$$\begin{cases} X_d(k+1) = A_d(\theta_d) \cdot X_d(k) + B_d(\theta_d) \cdot U_d(k) \\ Y_d(k) = C_d \cdot X_d(k) \end{cases} \tag{10}$$

where,

$X_d = [i_d \quad i_{1d} \quad i_{fe1d} \quad i_{fd}^*]^T$;

$U_d = [v_d^* \quad 0 \quad 0 \quad v_{fd}^*]^T$;

$Y_d = [i_d \quad i_{fd}^*]^T$;

$\theta_d = [R_a \quad R_{fd}^* \quad R_{1d} \quad R_{fe1d} \quad L_l \quad L_{ad} \quad L_{fd} \quad L_{1d} \quad L_{fe1d} \quad a]^T$;

For the q-axis model,

$$\begin{cases} X_q(k+1) = A_q(\theta_q) \cdot X_q(k) + B_q(\theta_q) \cdot U_q(k) \\ Y_q(k) = C_q \cdot X_q(k) \end{cases} \tag{11}$$

where,

$X_q = [i_q \quad i_{1q} \quad i_{2q} \quad i_{3q}]^T$;

$U_q = [v_q^* \quad 0 \quad 0 \quad 0]^T$;

$Y_q = [i_q]^T$;

$\theta_q = [R_a \quad R_{1q} \quad R_{2q} \quad R_{3q} \quad L_l \quad L_{aq} \quad L_{1q} \quad L_{2q} \quad L_{3q}]^T$;

Equations (10) and (11) constitute the de-coupled forms of equation (1). De-coupling the d- and q-axis equations facilitates de-coupled simulation of machine large disturbance responses. In the above formulation, the parameter matrices A and B are provided in Appendix A.2. The voltages v_d^* and v_q^* are defined as :

$$\begin{cases} v_d^* = v_d + \Phi_q \omega_r \\ v_q^* = v_q - \Phi_d \omega_r \end{cases} \tag{12}$$

For simulation purposes, the values of mutual inductances used in the machine models are obtained from neural network saturation models developed in the previous section. The values of R_a, R_{fd}^*, and a used in the machine model are from Table 1. The remaining rotor body parameters are assumed to be equal to values obtained from standstill time-domain testing of the test generator as described in reference [20]. In Figs. 6 and 7, currents recorded during large excitation disturbances are compared with simulated currents. Fig. 6

corresponds to the case when the generator is delivering 1000W of power with the field under-excited. Fig. 7 corresponds to the case when the generator is delivering 1750W of power with the field over-excited. Both tests are conducted at rated voltage.

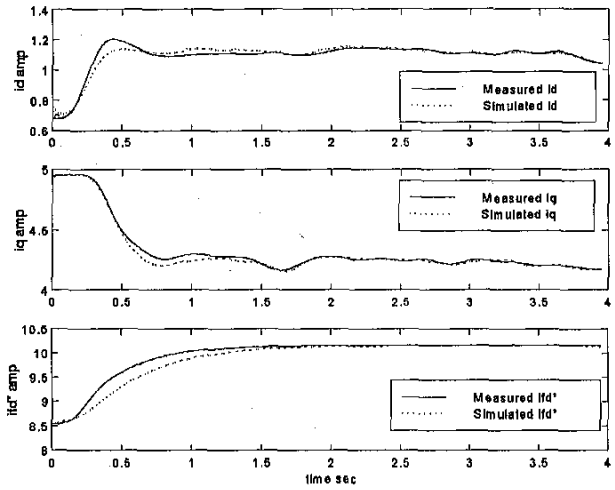

Fig. 6: Simulated and measured machine responses with generator delivering 1000W of power and field under-excited.

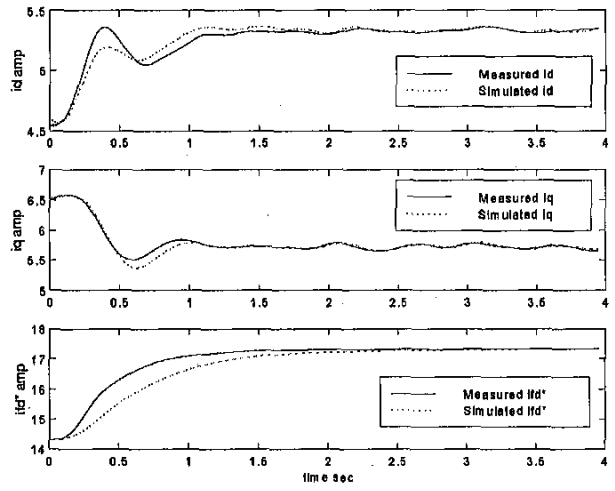

Fig. 7: Simulated and measured responses with generator delivering 1750W of power and field over-excited.

VII. CONCLUSIONS

Feed-forward multi-layer ANN based saturation models are established for a round rotor synchronous generator. Data for training the neural networks are acquired by conducting small excitation disturbance tests on a laboratory generator over a wide operating range. Small disturbance responses are used to estimate mutual inductances over the operating range of the generator. ANN saturation models are developed by mapping generator terminal variables to mutual inductances at various loading and excitation levels. Validation studies indicate that the established ANN rotor body models can correctly interpolate between patterns not used in the training process. It is anticipated that such models can readily be incorporated into existing transient stability programs to accurately account for generator saturation.

VIII. ACKNOWLEDGMENTS

This work is supported in part by the National Science Foundation, Grants ECS9625662 and ECS972284. The authors would like to thank Dr. Baj Agrawal and Mr. John Demcko of the Arizona Public Service Company for the use of their Power Angle Instrument.

IX. REFERENCES

[1] "IEEE Guide for Synchronous Generator Modeling Practices in Stability Analysis", *IEEE Std. 1110*, 1991.

[2] J. Lemay, T.H. Barton, "Small Perturbation Linearization of Saturated Synchronous Machine Equations", *IEEE Trans. Power Apparatus and Systems*, PAS-91, 1972, pp. 233-240.

[3] G. Shackshaft and P.B. Henser, "Model of Generator Saturation for use in Power System Studies", *Proc. IEE*, vol. 126, no. 8, 1979, pp. 759-763.

[4] El-Serafi A.M., Abdallah A.S., El-Sherbiny M.K., Badawy E.H., "Experimental Study of the Saturation and the Cross-Magnetizing Phenomenon in Saturated Synchronous Machines", *IEEE Trans. Energy Conversion*, Vol.EC-3, Dec. 1988, pp. 815-823.

[5] G. Shackshaft and R. Nielson, "Results of Stability Tests on an Under-Excited 120 MW Generator", *Proc. IEE*, vol. 119, 1972, pp. 175-188.

[6] de Mello F.P., and Hannett L.N., "Representation of Saturation in Synchronous Machines", *IEEE Trans. Power Systems*, v 1, Nov.1986, pp.8-14.

[7] A. M. El-Serafi and J. Wu, "Determination of the Parameters Representing the Cross-Magnetizing Effect in Saturated Synchronous Machines", *IEEE Trans. Energy Conversion*, v. 8, Sept. 1993, pp. 333-340

[8] Minnich, S.H., Schulz R.P., Baker D.H., Sharma D.K., Farmer R.G., Fish J.H., "Saturation Functions for Synchronous Generators from Finite Elements", *IEEE Trans. Energy Conversion*, v. 2, Dec. 1987, pp. 680-687.

[9] Boldea I., and Nassar S.A., "A General Equivalent Circuit (GEC) of Electric Machines including Cross-coupling Saturation and Frequency Effects", *IEEE Trans. Energy Conversion v. 3*, Sept. 1988, pp. 689-95.

[10] Marti J. R, and Louie K. W, "Phase-Domain Synchronous Generator Model Including Saturation Effects", *IEEE Trans. Power Systems*, v 12, n 1, Feb 1997. Pp. 222-229.

[11] J. Tamura and I. Takeda "A New Model of Saturated Synchronous Machines for Power System Transient Stability Simulations", *IEEE Trans. Energy Conversion*, vol. 10, no. 2, June 1995. Pp. 218-224.

[12] S. R Chaudhary, S. Ahmed-Zaid, N.A Demerdash, "An Artificial Neural Network Model for the Identification of Saturated Turbo-Generator Parameters Based on a Coupled Finite-Element/State-Space Computational Algorithm", *IEEE Trans. Energy Conversion*, v10, Dec. 1995, pp. 625-633.

[13] Wang J -C, Chaing H -D, Huang C- T, and Chen Y -T, "Identification of Synchronous Generator Saturation Based on On-line Digital Measurements", *IEE Proc. Generation, Transmission & Distribution*, v 142, n 3, May 1995, pp. 225-232.

[14] H. Tsai, A. Keyhani, J. A. Demcko, and D.A. Selin, "Development of a Neural Network Saturation Model for Synchronous Generator Analysis", *IEEE Trans. Energy Conversion* v 10 n 4 Dec 1995. pp. 617-624.

[15] S.-A. Tahan, I. Kamwa, "A Two-Factor Saturation Model for Synchronous Machines with Multiple Rotor Circuits", *IEEE Trans. Energy Conversion*, v10, n 4, December 1995. Pp. 609-616.

[16] R.E. Fairbairn and R.G. Harley, "On-line Measurement of Synchronous Machine Parameters", *IEEE Trans. Industry Applications*, v 28, n 3, May/June 1992.

[17] Chiang-Tsung Huang, Yung-Tien Chen, Chung-Liang Chang, Chung-Yi Huang, Hsiao-Dong Chiang and Jin-Cheng Wang, "On-line Measurement-Based Model Parameter Estimation for Synchronous Generators: Model Development & Identification Schemes", *IEEE Trans. Energy Conversion* v. 9 (June '94) pp.330-6.

[18] L. Xu, Z. Zhao, and J. Jiang,, "On-line Estimation of Variable Parameters of Synchronous Machines Using a Novel Adaptive Algorithm -- Estimation and Experimental Verification", *IEEE Trans. Energy Conversion*, Sept. 1997. v 12, n 3. pp. 200-210.

[19] H. Tsai, A. Keyhani, J.A Demcko, and R.G. Farmer, "On-line Synchronous Machine Parameter Estimation from Small Disturbance Operating Data", *IEEE Trans. Energy Conversion*, v10 n1, Mar. 1995. pp. 25-36

[20] S. Horning, A. Keyhani, I. Kamwa, "On-line Evaluation of a Round Rotor Synchronous Machine Parameter Set Estimated from Standstill Time-Domain Data", *IEEE Trans. Energy Conversion*, v 12, n 4, Dec 1997. pp. 289-296.

[21] J.L. Kirtley Jr., "On Turbine-Generator Rotor Equivalent Circuit Structures for Empirical Modeling of Turbine Generators", *IEEE Trans. PWRS-9*(1), 1994, pp.269-271.

[22] I.M Canay, "Causes of Discrepancies on Calculation of Rotor Quantities and Exact Equivalent Diagrams of the Synchronous Machine", *IEEE Trans. PWRS*, v PAS-88, n 7, July 1969. pp. 1114-1120.

[23] I. Kamwa, P. Viarouge, J. Dickinson, "Identification of Generalized Models of Synchronous Machines from Time-Domain Tests", *IEE Proc. C*, 138 (6), Nov. 1991. pp.485-498.

[24] I. Kamwa, and M Farzaneh,, "Data Translation and Order Reduction for Turbine-Generator Models used in Network Studies", *IEEE Trans. Energy Conversion*, v 12 n 2 June 1997, pp 118-126.

[25] Salon S. J., "Obtaining Synchronous Machine Parameters from Test", *Symposium on Synchronous Machine Modeling for Power Systems Studies*. Paper No. 83THO101-6-PWR. Available from IEEE Service Center, Piscataway, NJ, USA.

[26] J. Hertz, A. Krogh, and R.G. Palmer, *Introduction to the Theory of Neural Computation*, Addison Wesley Publishing Company, New York. 1993.

[27] K.S Narendra and K. Parthasarathy, "Identification and Control of Dynamical Systems Using Neural Networks", *IEEE Trans. Neural Networks*, v 1, pp. 4-27, 1990.

Appendix A

A.1 State Space Formulation for Determining Speed Voltages from Measurements

Machine speed ω_r in rad/sec can be computed from the equation $\omega_r \approx \omega_e + \dot{\delta}$ where ω_e is the synchronous speed in rad/sec, and δ is the measured rotor angle. Also,

$$A = \begin{bmatrix} 0 & \omega_r \\ -\omega_r & 0 \end{bmatrix} \quad ; \quad B \cdot U = \begin{bmatrix} v_d + R_a i_d \\ v_q + R_a i_q \end{bmatrix}$$

A.2 De-coupled State Space Representation of Model 3'.3

For the continuous case:

$$A^* = -L^{-1}R \; ; \; B^* = L^{-1}$$

where the L and R matrices for the d- axis circuit are shown below. A similar set of matrices may be developed for the q-axis.

$$R = diag([-R_a \quad R_{1d} \quad R_{fd1d} \quad R^*_{fd}]);$$

$$L = \begin{bmatrix} -(L_{ad}+L_l) & L_{ad} & L_{ad} & \frac{2}{3}aL_{ad} \\ -L_{ad} & L_{f1d}+L_{1d}+L_{ad} & L_{f1d}+L_{ad} & \frac{2}{3}a(L_{f1d}+L_{ad}) \\ -L_{ad} & L_{f1d}+L_{ad} & L_{fd1d}+L_{fd}+L_{f1d}+L_{ad} & \frac{2}{3}a(L_{fd}+L_{f1d}+L_{ad}) \\ -aL_{ad} & a(L_{f1d}+L_{ad}) & a(L_{fd}+L_{f1d}+L_{ad}) & \frac{2}{3}a^2(L_{fd}+L_{f1d}+L_{ad}) \end{bmatrix};$$

The discrete-time matrices parameter matrices A and B can be computed from A^* and B^*.

BIOGRAPHIES

Srinivas Pillutla received the B.E degree in Electrical Engineering from Bangalore University, Bangalore, India, in 1991. He obtained his MSEE from the Ohio State University, Columbus, OH in 1994. He is currently a Ph.D candidate in the Department of Electrical Engineering, The Ohio State University, Columbus, OH. Mr. Pillutla's research interests are in the areas of synchronous machine modeling, parameter estimation, and artificial neural network based system identification techniques.

Ali Keyhani received the Ph.D degree from Purdue University, West Lafayette, Indiana in 1975. From 1967 to 1969, he worked for Hewlett-Packard Co. on the computer-aided design of electronic transformers. From 1970 to 1973, he worked for Columbus and Southern Ohio Electric Co. on computer applications for power system engineering problems. In 1974, he joined TRW Controls and worked on the development of computer programs for energy control centers. From 1976 to 1980, he was a professor of Electrical Engineering at Tehran Polytechnic, Tehran, Iran. Currently, Dr. Keyhani is a Professor of Electrical Engineering at the Ohio State University, Columbus, Ohio. His research interests are in control and modeling, parameter estimation, failure detection of electric machines, transformers and drive systems.